

## Photooxidative Degradation of Dye Pollutants Accumulated in Self-Assembled Natural Polyelectrolyte Microshells under Visible Radiation

Xia Tao,\*<sup>[a]</sup> Jingmei Su,<sup>[a]</sup> and Jian-Feng Chen\*<sup>[b]</sup>

**Abstract:** A novel route to facilitate the degradation of dye pollutants, a class of well-known recalcitrant organic pollutants, is reported. This new approach is based on a natural polyelectrolyte microshell that was performed by the alternate adsorption of the anionic alginate sodium (ALG) and the cationic chitosan (CHI) onto weakly cross-linked melamine formaldehyde (MF) colloidal particles, and the subsequent sacrifice of MF templates in 0.1 M HCl. The as-prepared microshells could accumulate rhodami-

ne B (RhB) and fluorescein (Flu) efficiently in water under ordinary conditions by means of a simple mixing process. The photodegradation of the accumulated RhB and Flu was examined in the presence of Fe<sup>3+</sup> and H<sub>2</sub>O<sub>2</sub> under visible radiation. The accumulated RhB and Flu are rapidly degraded and the assembled shells maintain their

intact spherical shape throughout the photoreaction process. Results of recycling degradation experiments and the photochemical behavior of the shells, as demonstrated by confocal laser scanning microscopy (CLSM), UV-visible spectroscopy, and scanning force microscopy (SFM), further suggest that the constructed shells may be used as environmentally friendly microcontainers for the elimination of dyes in wastewater.

**Keywords:** dyes/pigments • microshells • photodegradation • pollutants • self-assembly

### Introduction

Dye pollutants in effluents from the textile and paper industries are a major source of environmental contamination, owing to their nonbiodegradability and toxicity.<sup>[1–3]</sup> The Fenton reaction (Fe<sup>2+</sup> or Fe<sup>3+</sup>/H<sub>2</sub>O<sub>2</sub>) as an economically attractive and environmentally benign choice has shown high efficiency in the degradation of organic pollutants.<sup>[4–6]</sup> In this process, active oxygen species with high oxidation activity, for example, hydroxyl radicals, hydroperoxyl radicals, and/or high-valence iron complexes, are involved.<sup>[7–10]</sup> However, use of the Fenton reaction to treat pollutants at lower concentrations suffers the drawback of an excessive loss of the active species generated prior to reacting with pollutants,

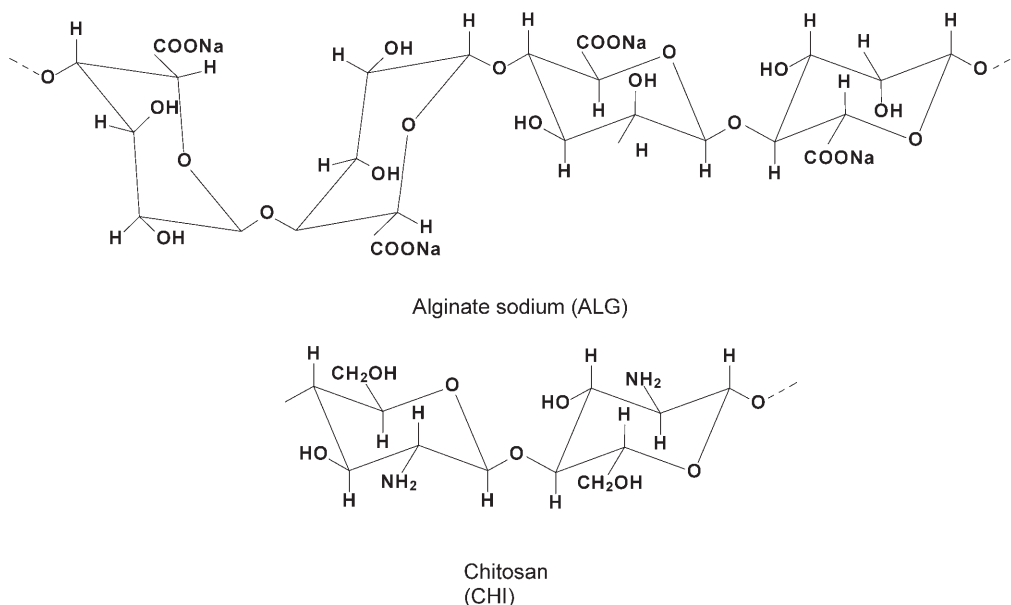
which results in increased wastewater-treatment costs. Thus, developing new strategies to utilize effectively the active species generated in the Fenton system for the treatment of pollutants remains a challenge.

Layer-by-layer (LbL) self-assembly<sup>[11]</sup> of oppositely charged polyelectrolytes onto dissolvable colloidal particles has been utilized in recent years to create ultrathin nano- and microshells with customized physicochemical properties. These assembled shells have been studied in many applications ranging from drug delivery to biomedical and materials science.<sup>[12,13]</sup> However, very few studies have been conducted that aim to use the nano- and micron-sized shells for the environmental treatment of organic pollutants in water. The hollow shells can provide a microcontainer for the treatment of dye pollutants in wastewater because they are composed of synthetic polyelectrolytes that are permeable to low-molecular-weight species, such as dyes, and can encapsulate the dye molecules in the interior of the shells in response to alterations in bulk pH values or salt concentrations.<sup>[12]</sup>

Here, we describe a novel route for the effective elimination of dye pollutants by introducing the assembled shells into dye-polluted systems. Firstly, we constructed a natural green polyelectrolyte (PE) microshell composed of alginate sodium (ALG) and chitosan (CHI) by using the LbL self-as-

[a] Prof. Dr. X. Tao, J. Su  
Key Lab for Nanomaterials of the Ministry of Education  
Beijing University of Chemical Technology, Beijing 100029 (China)  
Fax: (+86)10-6443-4784  
E-mail: taoxia@yahoo.com

[b] Prof. Dr. J.-F. Chen  
Research Center of the Ministry of Education for  
High Gravity Engineering and Technology  
Beijing University of Chemical Technology, Beijing 100029 (China)  
Fax: (+86)10-64448808  
E-mail: chenjf@mail.buct.edu.cn

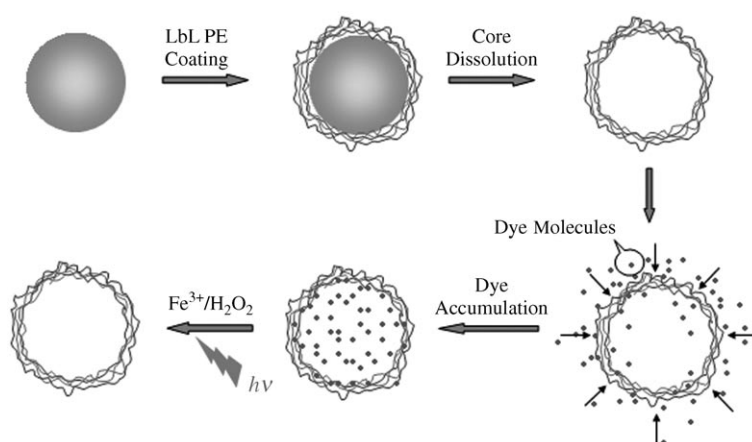


sembly technique. Subsequently, the constructed shells were used as carriers to accumulate dye pollutants in water. Preliminary results reported in a recent communication<sup>[14]</sup> showed that dye molecules can be accumulated inside the preformed microshells by a simple mixing process under moderate conditions, and in the visible-light-assisted Fenton system the accumulated dyes in defined regions can be degraded efficiently (Scheme 1). In this paper, rhodamine B (RhB), a stable laser dye was chosen as a representative target pollutant. The accumulation and photodegradation of RhB in the ALG/CHI shells was examined in more detail by confocal laser scanning microscopy (CLSM), UV-visible spectroscopy, and scanning force microscopy (SFM). For comparison, the photodegradation of another fluorescent dye, fluorescein (Flu), was also investigated. Of particular interest is that the constructed ALG/CHI shells, after completing the first accumulation and photodegradation, can be

reused. The changes in wall texture of the microshells prior to and after the photoreaction, as well as differences in the kinetics and adsorption amount in the recycling degradation are also discussed.

## Results and Discussion

**Preparation of natural microshells:** ALG and CHI were chosen as the wall components to build the microshells owing to their proven biocompatibility and safety.<sup>[15]</sup> Microelectrophoresis measurements were recorded to monitor the number of layers on weakly cross-linked melamine formaldehyde (MF) colloidal particles. Figure 1 shows the stepwise assembly of ALG and CHI on MF particles as variation in  $\zeta$  potentials. An initial value of approximately 47 mV corresponds to uncovered MF latex particles. The subsequent alternation in  $\zeta$  potentials observed with each coating step strongly suggest the multilayer growth of the assembled shells. Typically, five (ALG/CHI) bilayers were deposited, after which the MF templates were removed by exposure to HCl (pH 1). A CLSM image directly verified the successful assembly of the (ALG/CHI) shells templated onto MF colloidal particles (Figure 2). The fluorescent rings of the shells are formed by the fluorescein isothiocyanate (FITC)-labeled albumin. The assembled shells were found to maintain their intact



Scheme 1. The procedure for the visible-light-assisted degradation of dye pollutants accumulated in the natural polyelectrolyte microshells.

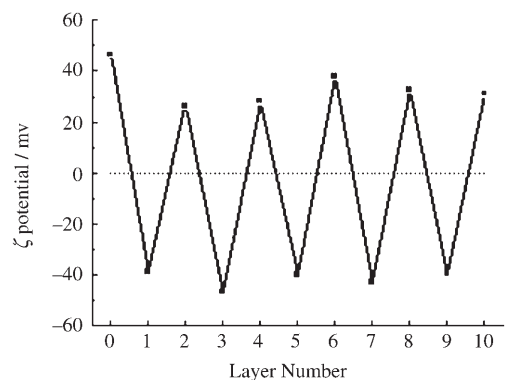


Figure 1. Plot of  $\zeta$  potential of ALG/CHI multilayers on 4.3  $\mu\text{m}$  MF latex particles as a function of the number of deposition steps. The uncovered MF latex particles exhibit a  $\zeta$  potential of approximately 47 mV.

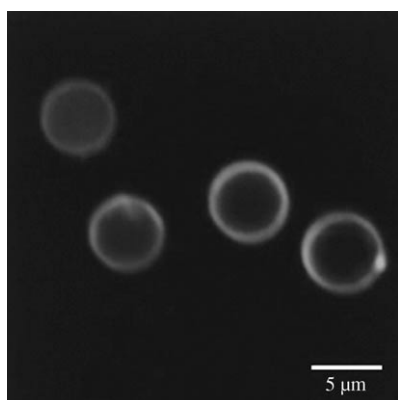


Figure 2. CLSM image of microspheres composed of (ALG/CHI)<sub>5</sub> templated onto 4.3  $\mu\text{m}$  MF particles, in which FITC-albumin was used to label the shells (FITC = fluorescein isothiocyanate).

spherical architecture after removal of the template and remained stable for at least one month.

**Accumulation of dyes in the microspheres:** The accumulation of dyes inside the assembled hollow shells was performed under moderate conditions by adding a suspension of the (ALG/CHI) shells to a solution of RhB or Flu overnight at room temperature. CLSM images verified directly the efficient accumulation of RhB and Flu in the interior of the (ALG/CHI) shells with almost complete integrity, yielding a higher concentration than in the bulk, as shown in Figure 3. As reported in a recent communication,<sup>[14]</sup> the accumulated amount of dye in a single shell composed of (ALG/CHI)<sub>5</sub> is  $6.0 \times 10^{-11}$  g for RhB and  $4.2 \times 10^{-11}$  g for Flu, which corresponds to  $7.5 \times 10^{10}$  RhB molecules and  $6.7 \times 10^{10}$  Flu molecules.

**Degradation of dyes:** After simple separation by filtration, the dye-accumulating microspheres were dispersed in the Fenton reagent. Figure 4 shows the degradation of the accumulated RhB under various conditions. After 45 min of visible radiation, the accumulated RhB in the  $\text{Fe}^{3+}$  solution was

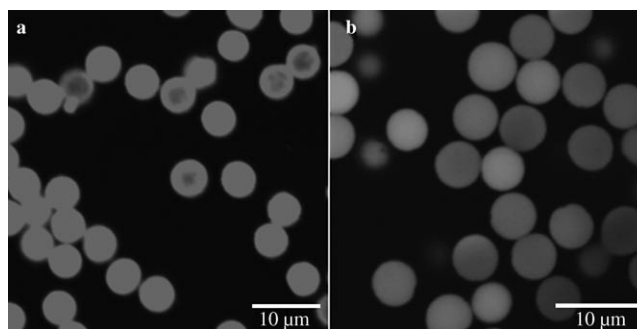


Figure 3. CLSM images of the (ALG/CHI) shells accumulating RhB (a) and Flu (b).

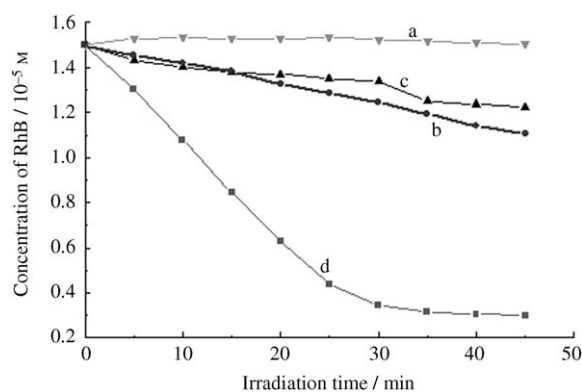


Figure 4. Changes in concentration of the accumulated RhB (15  $\mu\text{M}$ ) as a function of radiation time under different conditions. a) Solution of the accumulated RhB and  $\text{Fe}^{3+}$  (0.2 mM) under visible radiation; b) solution of the accumulated RhB and  $\text{H}_2\text{O}_2$  (0.5 mM) under visible radiation; c) accumulated RhB in the presence of  $\text{Fe}^{3+}$  and  $\text{H}_2\text{O}_2$  in the dark; d) accumulated RhB in the presence of  $\text{Fe}^{3+}$  and  $\text{H}_2\text{O}_2$  under visible radiation.

scarcely decomposed (curve a), and slightly decomposed in the presence of  $\text{H}_2\text{O}_2$  (curve b). If both  $\text{Fe}^{3+}$  and  $\text{H}_2\text{O}_2$  were present, approximately 18% of the accumulated RhB disappeared after reaction for 45 min in the dark (curve c). In contrast, under the same conditions as (c), but with visible illumination, approximately 80% of the accumulated RhB was degraded (curve d). Evidently, visible radiation accelerated considerably the degradation process. In addition, the rate of photodegradation of RhB accumulated inside the microspheres is slightly slower than that of free RhB in the homogeneous  $\text{Fe}^{3+}/\text{H}_2\text{O}_2$  solution. This is understandable because, according to Serpone et al. in a review of processes occurring in confined spaces,<sup>[16]</sup> the photoreaction kinetics in restricted spaces, that is, dye molecules in the microspheres and the Fenton reagent in the aqueous phase, are different from those in a completely free space. Furthermore, the nanometer-sized polyelectrolyte microspheres might block to some extent the visible-light radiation, thereby leading to the decrease in photoefficiency.

Direct visualization on the changes in the accumulated dyes inside the shells before and after the photoreaction was traced by CLSM. Figure 5 displays CLSM fluorescence

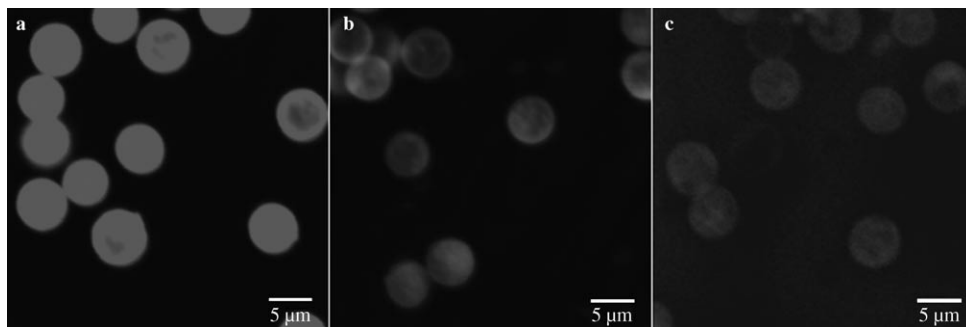


Figure 5. Variations in CLSM of the (ALG/CHI)<sub>5</sub> shells accumulating RhB (15 μM) in the presence of Fe<sup>3+</sup> (0.2 mM) and H<sub>2</sub>O<sub>2</sub> (0.5 mM) before (a) and after irradiation for 45 (b) and 60 min (c).

images of the (ALG/CHI)<sub>5</sub> shells accumulating RhB in the presence of Fe<sup>3+</sup> and H<sub>2</sub>O<sub>2</sub> before (a) and after irradiation for 45 (b) and 60 min (c). The fluorescence intensity in the shell interior, which is proportional to the RhB concentration, decreases rapidly as the visible radiation increases. In addition, we used CLSM to examine the photodegradation of the accumulated Flu inside the shells in the Fenton reagent (Figure 6). A CLSM transmission image instead of a

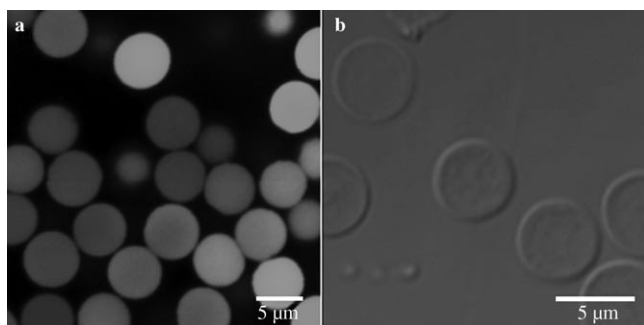


Figure 6. CLSM images of the (ALG/CHI)<sub>5</sub> shells accumulating Flu (10 μM) in the presence of Fe<sup>3+</sup> (0.2 mM) and H<sub>2</sub>O<sub>2</sub> (0.5 mM) before (a) and after irradiation for 30 min (b). Note: fluorescence image (a); transmission image (b).

CLSM fluorescence image is displayed in Figure 6b because the fluorescence intensity of the Flu-accumulating shells, after the photoreaction for 30 min, was extremely weak. This also suggests that the accumulated Flu can be photodegraded at a fast rate in the Fenton system. In addition, during the whole photodegradation reaction, no fluorescence was observed in the bulk solution, which means that the dye molecules are located well inside the shells. Moreover, because the wall of the shells is permeable to Fenton reagent, the photoreaction process can be deduced to take place within the microshells rather than in the bulk solution.

To gain further insight into changes in the wall texture of the nano- and microshells in diverse cases, the SFM technique can be employed.<sup>[17]</sup> Figure 7 shows SFM images of the air-dried hollow (ALG/CHI)<sub>5</sub> shell (a), the RhB-accumulating (ALG/CHI)<sub>5</sub> shell (b), and the RhB-accumulating (ALG/CHI)<sub>5</sub> shell after the photoreaction (c).

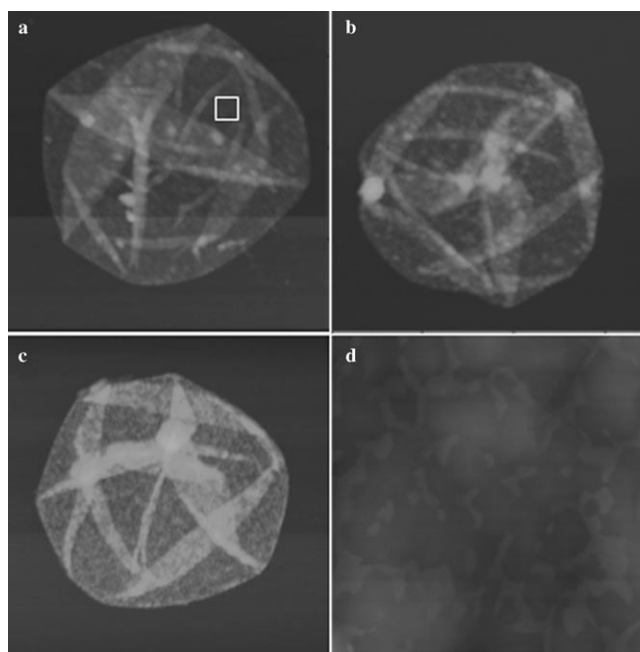


Figure 7. SFM images of the air-dried (ALG/CHI)<sub>5</sub> shell (a), RhB-accumulating (ALG/CHI)<sub>5</sub> shell (b), and RhB-accumulating (ALG/CHI)<sub>5</sub> shell after 60 min of visible radiation in a solution of Fe<sup>3+</sup> (0.2 mM) and H<sub>2</sub>O<sub>2</sub> (0.5 mM) (c). d) HR-SFM image of the area 300 nm × 300 nm marked in (a) showing the surface texture of the (ALG/CHI)<sub>5</sub> microshell free of folds.

ure 7a, b, and c gave values of  $\sim 3.4 \pm 0.5$  nm,  $4.5 \pm 0.5$  nm, and  $7.4 \pm 0.5$  nm, respectively. Compared with the hollow (ALG/CHI) shells, no apparent change in surface-wall texture occurs upon accumulation of the shells with RhB, whereas after the photoreaction, an obvious enhancement in the RhB-accumulating shell wall is observed. A similar enhancement in the surface roughness of the microshells caused by the photochemical reaction was also observed by assembling a Congo red dye onto the surface of the polyelectrolyte shells and inducing a photoreaction by applying visible radiation.<sup>[18]</sup>

**Recycled accumulation and degradation:** Because the (ALG/CHI) shells can be easily recovered by filtration, we carried out two consecutive photodegradations of RhB with

the (ALG/CHI) shells as the microcontainers. The (ALG/CHI) shells were reutilized repetitively after the color attributed to the RhB in the shell interior disappeared completely. Figure 8 shows the photoreaction kinetics in two

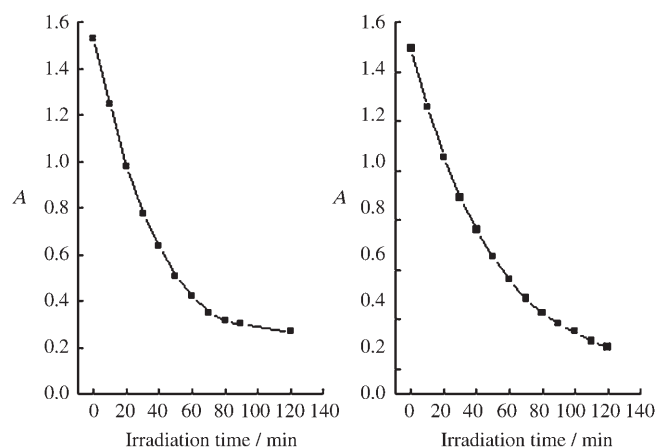


Figure 8. Recycling degradation of RhB (25  $\mu\text{M}$ ) accumulated in the (ALG/CHI) shells in the presence of  $\text{Fe}^{3+}$  (0.2 mM) and  $\text{H}_2\text{O}_2$  (0.5 mM) under visible radiation. Left: first round; right: second round.

rounds of recycling degradation. The kinetics of the two sets of data are not totally uniform, namely, the rate of the first round is faster than that of the second, and the accumulated amount of RhB in the second recycling run is slightly lower than that in the first run (see below for discussion of the photoreaction process occurring in defined microshells).

Microscopy observations of the RhB-accumulating shells in two repeated experiments were obtained by CLSM. Figure 9 shows CLSM images of the RhB-accumulating shells prior to (a, c) and after (b, d) the photoreaction. Likewise, we recorded CLSM transmission images to reveal changes in morphology of the shells after exposure to visible radiation, exhibited as faint fluorescence of the shell interior. Apparently, the accumulated RhB can be efficiently degraded in every run.

Additionally, we measured the total amount of iron present in the bulk solution after the first photodegradation by using a modified 1,10-phenanthroline method.<sup>[19]</sup> The result shows that approximately 75% of the added iron ions are in the supernatant liquid, which means that a certain proportion of iron ions exists in the microshells. Also, due to the restricted space of the microshells, the intermediates and products produced during the photoreaction are unlikely to enter into the bulk solution completely. Thus, the existence of these species, such as iron ions, as well as the intermediates and products produced in the microshells may lead to 1) the wall-texture changes of the microshells prior to and after the photoreaction (Figure 7), 2) the decrease in the amount of dye adsorbed in the recycling experiment, and 3) the differences in the kinetics in the two recycling photodegradation reactions (Figure 8). Importantly, during the whole process of the accumulation and subsequent photode-

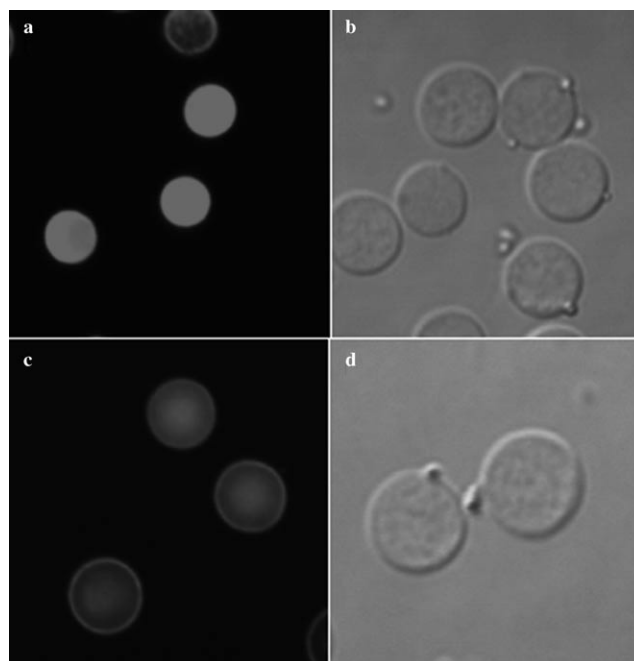


Figure 9. CLSM images of the RhB-accumulating shells before (a, c) and after (b, d) the photoreaction for 120 min: (a) and (b) correspond to the first accumulation and subsequent degradation, (c) and (d) correspond to the second accumulation and subsequent degradation.

gradation of dyes, the constructed (ALG/CHI) microshells are quite stable and retain their intact spherical shape, which indicates that the shells are stable against attack from highly active species generated during a photoassisted Fenton reaction.

## Conclusion

This work introduces a novel route, based on assembled natural polyelectrolyte microshells, for the treatment of dye pollutants in water. UV-visible spectra, CLSM, and SFM were employed to verify the efficient degradation of dye pollutants in defined microregions. This approach is significant for several reasons: 1) it allows the accumulation of a variety of dye pollutants under moderate conditions in shells comprised of natural polyelectrolytes, 2) the photodegradation reaction can proceed in aqueous media without addition of other organic reagents, and 3) the assembled shells possess good photostability. Further, due to the tailored shell thickness on a nanometer scale as well as the ordered shell composition and the versatility of the LbL method, this technique is likely to be extended to heterogeneous photocatalytic reactions for the remediation of organic pollutants in aqueous ecosystems.

## Experimental Section

**Materials:** ALG ( $M_w = 12000\text{--}80000$ ) was obtained from Sigma, Canada. CHI ( $M_w = 30000$ ) was obtained from Primex Biochemicals, Norway. MF particles ( $4.31 \pm 0.18 \mu\text{m}$ ) were purchased from Microparticles, Germany. FITC-albumin was purchased from Sigma. RhB and Flu were of analytical reagent grade and were used without further purification. All chemicals were used as received. Millipore water was used throughout the study.

**Procedure for the assembly of the hollow and dye-accumulating shells:** 1.5 mL of alginate solution ( $1 \text{ mg mL}^{-1}$  in  $0.5 \text{ M NaCl}$ ) or 1.5 mL of chitosan solution ( $1 \text{ mg mL}^{-1}$  in  $0.2 \text{ M NaCl}$  at pH 3.8), with a charge opposite to that of either MF templates or the last layer deposited, was added to a template colloidal solution (0.3 mL) and left to absorb for 1 h. The excess of added species was removed after each layer was deposited by performing three centrifugation (2500 g, 3 min)/washing/redispersion cycles with dilute aqueous NaCl. Subsequent layers were deposited until the desired number of multilayers was achieved. Hollow shells were obtained by dissolving the MF cores with HCl (0.1 M, 30 min), centrifuging (2500 g, 2 min), and washing three times with water.

Equal amounts of a microshell suspension (aged for approximately two days) and a dye solution were mixed together overnight. The filled shells were rinsed with Millipore water until no dye in the supernatant solution was detected by UV/Vis measurements.

**Photoreactor and light source:** A 500 W halogen lamp (Institute of Electric Light Source, Beijing) was positioned inside a cylindrical Pyrex vessel surrounded by a jacket with circulating water (Pyrex) to cool the lamp. A light filter was used to eliminate wavelengths of less than 420 nm.

**Procedures and analyses:** All radiation experiments were performed by using a quartz cell with an appropriate stirrer. At given radiation time intervals, samples (4 mL) at an initial pH of 2.5 were removed and analyzed by observation of variations in UV/Vis spectra by using a Lambda Bio 20 spectrophotometer (Perkin-Elmer).

Multilayer growth of the assembled hollow shell wall on MF particles was monitored by measuring the microelectrophoretic mobility of the coated particles with a Malvern Zetasizer HAS 3000, by taking the average of ten measurements at the stationary level. The mobility ( $u$ ) was converted into the zeta potential ( $\zeta$ ) by using the Smoluchowski relation ( $\zeta = u\eta/\epsilon$ ), in which  $\eta$  and  $\epsilon$  are the viscosity and permittivity of the solution, respectively.

Confocal micrographs were taken by using a LSM 510 confocal microscope (Carl Zeiss) equipped with multiple laser lines from UV to infrared for excitation of fluorophores. The optical parameters of the CLSM remained unchanged prior to and after the photoreaction so that the measured intensities could be compared quantitatively.

The scanning force microscopy (SFM) images were recorded at ambient temperature by using a Digital Instrument Nanoscopy IIIa in the tapping mode. Samples were prepared by applying a drop of the shell solution onto a freshly cleaved mica substrate. After the shells were allowed to settle, the substrate was extensively rinsed with Millipore water and then dried under a gentle stream of nitrogen.

## Acknowledgements

This work was supported financially by the National Natural Science Foundation of China (No. 20577002, 20546001, and 20325621) and the Talent Program of Beijing University of Chemical Technology.

- [1] S. Horikoshi, A. Saitou, H. Hidaka, N. Serpone, *Environ. Sci. Technol.* **2003**, *37*, 5813–5822.
- [2] a) W. Zhao, W. Ma, C. Chen, J. Zhao, Z. Shuai, *J. Am. Chem. Soc.* **2004**, *126*, 4782–4783; b) F. Chen, Y. Xie, J. He, J. Zhao, *J. Photochem. Photobiol. A* **2001**, *138*, 139–146.
- [3] C. Hu, J. C. Yu, Z. Hao, P. K. Wong, *Appl. Catal. B* **2003**, *40*, 131–140.
- [4] O. Legrini, E. Oliveros, A. M. Braun, *Chem. Rev.* **1993**, *93*, 671–698.
- [5] J. Fernandez, M. R. Dhananjeyan, J. Kiwi, Y. Semuna, J. Hilborn, *J. Phys. Chem. B* **2000**, *104*, 5298–5301.
- [6] M. Cheng, W. Ma, J. Li, Y. Huang, J. Zhao, *Environ. Sci. Technol.* **2004**, *38*, 1569–1575.
- [7] D. T. Sawyer, J. S. Valentine, *Acc. Chem. Res.* **1981**, *14*, 393–400.
- [8] J. Kiwi, A. Lopez, V. Nadtochenko, *Environ. Sci. Technol.* **2000**, *34*, 2162–2168.
- [9] C. Walling, *Acc. Chem. Res.* **1975**, *8*, 125–131.
- [10] a) X. Tao, W. Ma, T. Zhang, J. Zhao, *Angew. Chem.* **2001**, *113*, 3103–3105; *Angew. Chem. Int. Ed.* **2001**, *40*, 3014–3016; b) F. Chen, W. Ma, J. He, J. Zhao, *J. Phys. Chem. A* **2002**, *106*, 9485–9490.
- [11] a) G. Decher, *Science* **1997**, *277*, 1232–1237; b) S. W. Keller, S. A. Johnson, E. S. Brigham, E. H. Yonemoto, T. E. Mallouck, *J. Am. Chem. Soc.* **1995**, *117*, 12879–12880; c) J. Ruths, F. Essler, G. Decher, H. Riegler, *Langmuir* **2000**, *16*, 8871–8878.
- [12] a) Z. Dai, H. Möhwald, *Chem. Eur. J.* **2002**, *8*, 4751–4755; b) Z. Dai, L. Dähne, H. Möhwald, B. Tiersch, *Angew. Chem.* **2002**, *114*, 4191–4194; *Angew. Chem. Int. Ed.* **2002**, *41*, 4019–4022.
- [13] A. D. Dinsmore, M. F. Hsu, M. G. Nikolaidis, M. Marquez, A. R. Bausch, D. A. Weitz, *Science* **2002**, *298*, 1006–1009.
- [14] X. Tao, J. Su, J. Chen, Zhao, *Chem. Commun.* **2005**, 4607–4609.
- [15] a) S. Miyazaki, A. Nakayama, M. Oda, M. Takada, D. Attwood, *Biol. Pharm. Bull.* **1994**, *17*, 745–747; b) X. L. Yan, E. Khor, L. Y. Lim, *J. Biomed. Mater. Res.* **2001**, *58*, 358–365; c) O. Gaserod, A. Sannes, G. Skjak-Braek, *Biomaterials* **1999**, *20*, 773–783.
- [16] R. F. Khairutdinov, N. Serpone, *Prog. React. Kinet.* **1996**, *21*, 1–68.
- [17] a) M. Matsumoto, D. Miyazaki, M. Tanaka, R. Azumi, E. Manda, Y. Kondo, N. Yoshino, H. Tachibana, *J. Am. Chem. Soc.* **1998**, *120*, 1479–1484; b) I. Gössl, L. Shu, A. D. Schlüter, J. P. Rabe, *J. Am. Chem. Soc.* **2002**, *124*, 6860–6865.
- [18] X. Tao, J. Li, H. Möhwald, *Chem. Eur. J.* **2004**, *10*, 3397–3403.
- [19] W. Song, W. Ma, J. Ma, C. Chen, J. Zhao, *Environ. Sci. Technol.* **2005**, *39*, 3121–3127.

Received: November 23, 2005  
Published online: March 10, 2006